Adsorption Properties and Microporous Structure of Adsorbents Produced from Phenolic Resin and Biomass

J. SIMITZIS,* J. SFYRAKIS, and A. FALIAGAS

National Technical University of Athens, Department of Chemical Engineering, Laboratory of Special Chemical Technology, 9 Heroon Polytechniou Str., Zografou Campus, GR-157 80 Athens, Greece

SYNOPSIS

Mixtures of novolac resin and olive stone biomass in proportions 20 : 80 (w : w) are cured, pyrolyzed up to 1000°C (material C20), and activated with steam (material C20a). The adsorption properties of these materials and a commercial activated carbon (CC) are investigated based on the adsorption of nitrogen and pentane. The adsorption capacity, the surface area determined by the BET and DRK equation, and the pore volume determined as micropore volume by the DR equation, and as cumulative pore volume related to the Kelvin equation, for the materials follow the order C20a > CC > C20. The DR equation can be applied for the adsorption of nitrogen on the materials examined in the region of P/P_o = 0.005 up to 0.3 that exceeds in both sides the common range for the applicability of the DR equation. The activated materials C20a and CC are mainly microporous and reveal the type I isotherms of the Brunauer classification for nitrogen adsorption. The only pyrolyzed material, C20, contains both micropores and mesopores and reveals characteristics of both types I and II. The number of layers for C20a and CC is lower than 2 and for C20 is more than 2. © 1995 John Wiley & Sons, Inc.

INTRODUCTION

Adsorption on suitable carbonaceous materials has been extensively used both as an independent process and in combination with other techniques in a wide range of separation processes. Techniques that have been successfully used in combination with adsorption include biological degradation used for the removal of a broad spectrum of hazardous compounds from contaminated wastewaters.[1,2] Distillation used in combination with adsorption is the most promising hybrid process for the separation of mixtures such as propane and propylene.[3,4] For wastes with high metal concentrations, precipitation processes are the most economical. However, the effectiveness of the process is increased with additional treatment processes such as adsorption by activated carbons. The ability of activated carbons to remove heavy metals from aqueous wastes and for drinking water has been investigated.[5,6] Novel processes such as the combination of supercritical extraction with adsorption have been proposed for the remediation of soils contaminated with heavy molecular weight organic compounds.[7]

Commercially available activated carbons are produced from carbonaceous raw materials such as coals, peat, wood, coconuts, and petroleum coke with a suitable thermal or chemical activation process.[8,9] Carbonaceous adsorbents with modified properties can be obtained by carbonization of synthetic polymeric materials such as macroreticular styrene/divinyl benzene copolymers, which have been used for the treatment of wastewater.[8,10] Carbon molecular sieves have been prepared by pyrolysis of polymers such as polyvinylidene chloride (PVDC), Saran, polyphenylenes, and phenol-formaldehyde resins,[11-13] or by pyrolysis of coal followed by special treatment.[14,15] Agricultural waste by-products, e.g., olive stones, almond shells, peanut hulls, etc., have been used for the production of low-cost adsorptive materials that have useful properties such as appropriate hardness, very low ash content, and near absence of sulfur.[16-20]

* To whom correspondence should be addressed.

Journal of Applied Polymer Science, Vol. 58, 541-550 (1995)
 CCC 0021-8995/95/030541-10

Table I Raw Material Composition, Processes for Production of Adsorbents, and Their Shapes

			Processes			
No.	Symbol	Raw Materials N/B (w/w)	Curing (170°C, 0.5 h)	Carbonization (T_{max}, t_T, h.r.)	Activation (by Steam at 930°C)	Form of Product
1	C20	20/80	Yes	1000°C, 10 min, 4°C/min	No	Small cylinders
2	C20a	20/80	Yes	1000°C, 10 min, 4°C/min	Yes	Small cylinders
3	CC	Commercial activated carbon (mainly for industrial use)				Granules

N, novolac; B, biomass; T_{max}, maximum temperature; t_T, residence time at maximum temperature; h.r., heating rate.

Carbonaceous adsorbents have been produced by the pyrolysis of composites prepared from phenolic resin (type novolac) (NR) with olive stone biomass (OSB),[21–26] cottonseed,[27,28] and lignite[29] as well as from furfuryl alcohol-formaldehyde resin and OSB.[30] Adsorbents produced from a 20 : 80 (w : w) mixture of NR : OSB and pyrolyzed at 1000°C show the highest uptake of toluene and cyclohexane from the vapor phase when compared with products obtained from different compositions or carbonization temperatures.[31]

The present work concerns the adsorption properties and the microporous structure of adsorbents produced from NR and OSB including their comparison to commercial adsorbent. As adsorbants nonpolar substances are chosen, viz., nitrogen and pentane.

EXPERIMENTAL

Adsorbent Preparation

Carbonaceous adsorbents were produced from NR and biomass in proportions 20 : 80 (w : w). The resin was prepared from the polymerization of phenol with formaldehyde in proportions 1.22 : 1 (mol : mol) with oxalic acid as catalyst in proportion 1.5% w : w phenol after which the resin was separated, dried, and pulverized. Biomass consisted of the agricultural/industrial by-product that is left from olives after pressing and separation of the oil. It was dried, ground, and sifted to yield grains with a diameter less than 300 μm. Hexamethylenetetramine (viz., hexa) was used in proportion 7 : 2 novolac : hexa (w : w) to cure mixtures of novolac with biomass at 170°C for 30 min. Carbonization of the cured materials was accomplished in a cylindrical tube oven under the continuous flow of N_2. The oven was heated to 1000°C at the rate of 4°C/min, after which the samples remained in the oven for a further 10 min, were subsequently cooled to room temperature, and kept under vacuum. Further, pyrolysis residues were activated with steam at 930°C.

Characterization by Sorption

The adsorbents produced by carbonization, the activated materials, and the commercial product that was used in the present work for comparison purposes, were degassed prior to use under vacuum at 200°C for 3 h. Pentane used for the vapor phase adsorption was reagent grade. For the vapor phase adsorption experiments a quartz spring apparatus including a Griffin and George cathetometer was used. This apparatus is described in detail elsewhere.[32,33] All sorption experiments were conducted at 20°C and relative pressure P/P_o = 0.1 where P_o is the saturation pressure of the vapor at this temperature.

Nitrogen adsorption experiments and the measurements of the nitrogen adsorption isotherms were performed at −196°C using the SORPTOMATIC (series 1800) apparatus of Carlo Erba Strumentazione. The samples were previously dried at 120°C and outgassed to less than 0.5 torr for about 1 h in an outgassing unit made by Carlo Erba Strumentazione.

RESULTS

Table I shows the adsorptive materials, C20 and C20a, prepared by carbonization without or with activation, respectively, as well as the commercial activated carbon, CC (Acticarbone, grain diameter ~ 1.5 mm, specific surface area 500 m^2/g). The form of the products given in Table I were used for all adsorption experiments.

Figure 1 shows the adsorption isotherms of N_2 for the adsorbents of Table I where the materials C20a and CC have a rapid rise in the amount of the adsorptive substance. In all isotherms a "knee" is observed, steeper for C20a and CC at low relative pressure (less than $P/P_o = 0.1$). Nitrogen adsorption isotherms were followed up to relative pressure near the saturation one (about $P/P_o = 1$). The activated carbon C20a shows the highest N_2 uptake in comparison to the nonactivated C20 and the commercial product CC.

Figure 2 shows the pentane uptake versus time for the adsorbents of Table I. The obtained curves show initially a strong increase up to about 30 min, after which they are gradually stabilized at about t = 60 min to their equilibrium values. The behavior of all three adsorbents against both adsorbates N_2 and pentane are qualitatively similar, comparing the corresponding equilibrium uptakes. It is apparent from Figures 1 and 2 that the relative order of the adsorbents with respect to increasing vapor uptake is in both cases the same:

$$\text{C20a} > \text{CC} > \text{C20}.$$

For any point $i(P_i/P_o, V_i)$ on the isotherm of Figure 1 the volume W_i of the pores is calculated[34,35]:

$$W_i = n_i/\rho^* \tag{1}$$

and

$$n_i = V_i/22414 \tag{2}$$

where V_i and P_i are the gas volume adsorbed and the pressure at any point i; W_i is the amount adsorbed expressed as a liquid volume at any point i; ρ^* is the density of the adsorbate in the micropores (at temperatures well below the critical point, e.g., near the boiling point of the adsorptive, ρ^* may be taken as equal to the ordinary density ρ_L of the bulk liquid adsorptive); and n_i are the moles of adsorbate per gram of adsorbent.

The micropore volume can be determined according to the Dubinin–Radushkevich equation (DR plot)[34–37]:

$$\log W = \log W_o - D \log^2\left(\frac{P}{P_o}\right) \tag{3}$$

where P_o is the saturation pressure, D is a constant, and W_o is the total micropore volume according to the DR equation.

The plot of the log W of the N_2 uptake versus the $\log^2(P/P_o)$ for the curves of Figure 1 is shown in Figure 3. The W_o is determined from the intercept of the straight line portion of the curve.

Mesopore size calculations are usually made with the aid of the Kelvin equation in the form[34,35]:

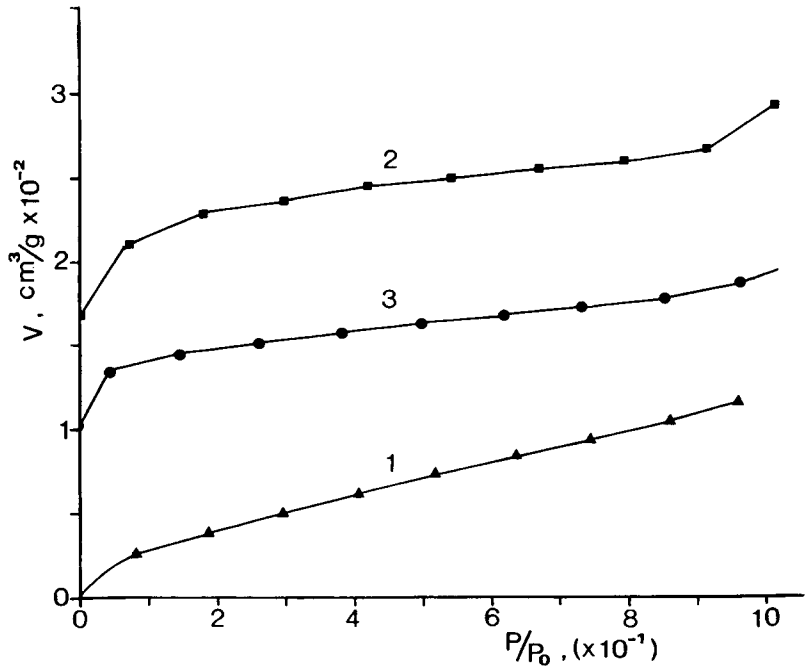

Figure 1 Adsorption isotherms of N_2 for adsorbents of Table I: V, volume uptake per mass unit; P, pressure; P_o, saturation pressure. (1) C20, (2) C20a, (3) CC (Table I).

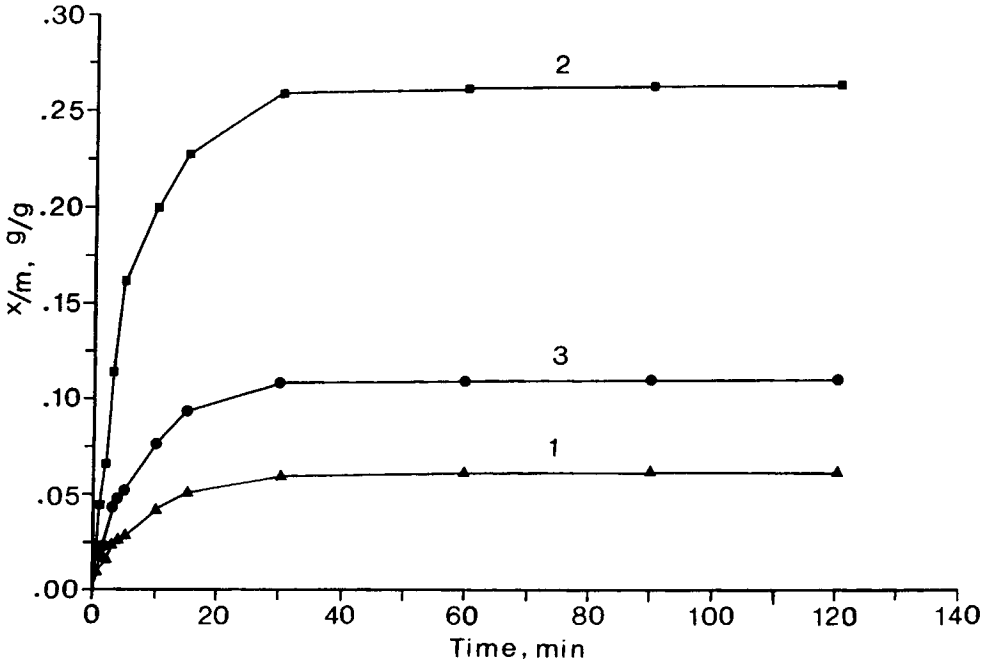

Figure 2 Adsorption of pentane versus time: x, adsorbed amount of vapor and m, amount of adsorbent. (1) C20, (2) C20a, (3) CC (Table I).

$$\ln\frac{P}{P_o} = -\frac{2\sigma V_L}{RTr_m} \tag{4}$$

σ and V_L are the surface tension and molar volume of the condensed liquid adsorbate, respectively ($V_L = 1/\rho^*$); P/P_o is the relative pressure of vapor in equilibrium with a meniscus having a radius of curvature r_m (the pore radius of curvature); r_m includes the pores with radius $\leqq r_i$ (for any point i corresponding to volume W_i; R is the gas constant; T is equal to 77.35 K (for the measurements with nitrogen).

The obtained results are represented graphically in Figure 4 based on the experimental data of Figure 1.

The commonly used methods for surface area determination involve adsorption when it starts to level out around the monolayer region. According to the Brunauer–Emmett–Teller (BET) equation[34,35]:

$$\frac{P/P_o}{V(1 - P/P_o)} = \frac{1}{V_m c} + \frac{c - 1}{V_m c}(P/P_o) \tag{5}$$

where V and P are the corresponding volume V_i and pressure P_i at any point; V_m is the volume of gas adsorbed when the adsorbent surface is covered with a unimolecular layer and is termed the monolayer; and C is a constant related to the heat of adsorption.

By plotting the left function of the above equation versus P/P_o, a straight line results with slope $s = (C - 1)/V_m C$ and intercept $i = 1/V_m C$. The solution of both equations gives the values of V_m and C.

The pore specific surface area of the adsorbents can be calculated from the equation[34,35]:

$$A_p = n_m a_m L \tag{6}$$

where n_m for nitrogen (volumetric measurements) is $n_m = V_m/22414$ and for pentane (gravimetric measurements) is $n_m = X_m/M$; V_m is determined by the BET equation; X_m is the monolayer capacity in grams of adsorbate per gram solid adsorbent (i.e. equilibrium value for the pentane adsorption); M is the molecular weight of the adsorbate; a_m is the average area occupied by a molecule of the adsorbate in a completed monolayer; and L is the Avogadro constant.

According to Mikhail and Robens,[35] the values of a_m are 0.162 and 0.37 nm^2 for nitrogen and pentane, respectively.

Alternatively, the specific surface area, which corresponds to micropores, can be calculated by the Dubinin–Radushkevich–Kaganer equation (DRK plot)[34,35]:

$$\log V = \log V_m - D_1 \log^2\left(\frac{P}{P_o}\right). \tag{7}$$

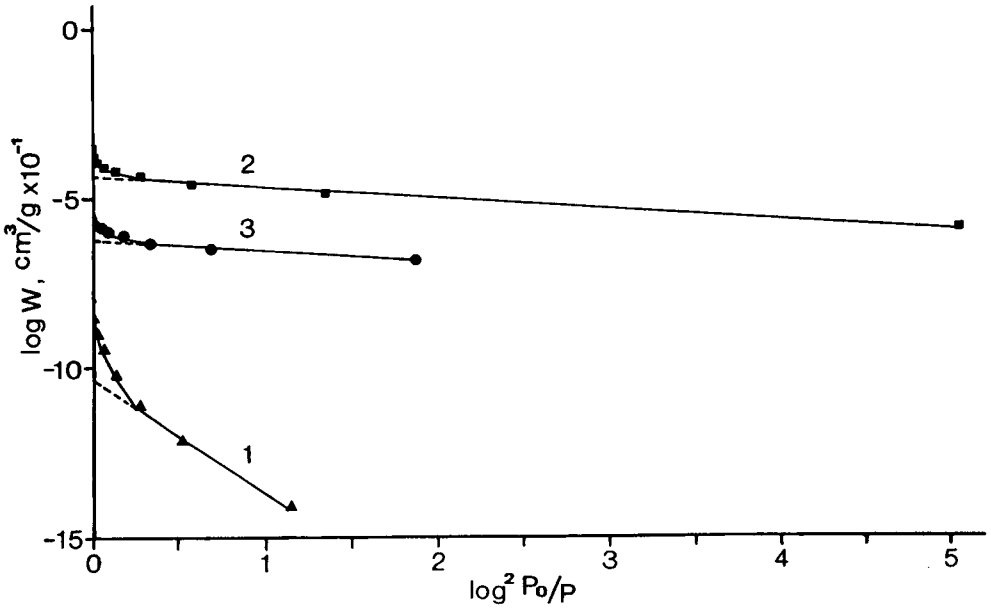

Figure 3 Logarithm plot of N_2 uptake according to the DR equation (see text): W, liquid volume uptake per mass unit; P, pressure; P_o, saturation pressure. (1) C20, (2) C20a, (3) CC (Table I).

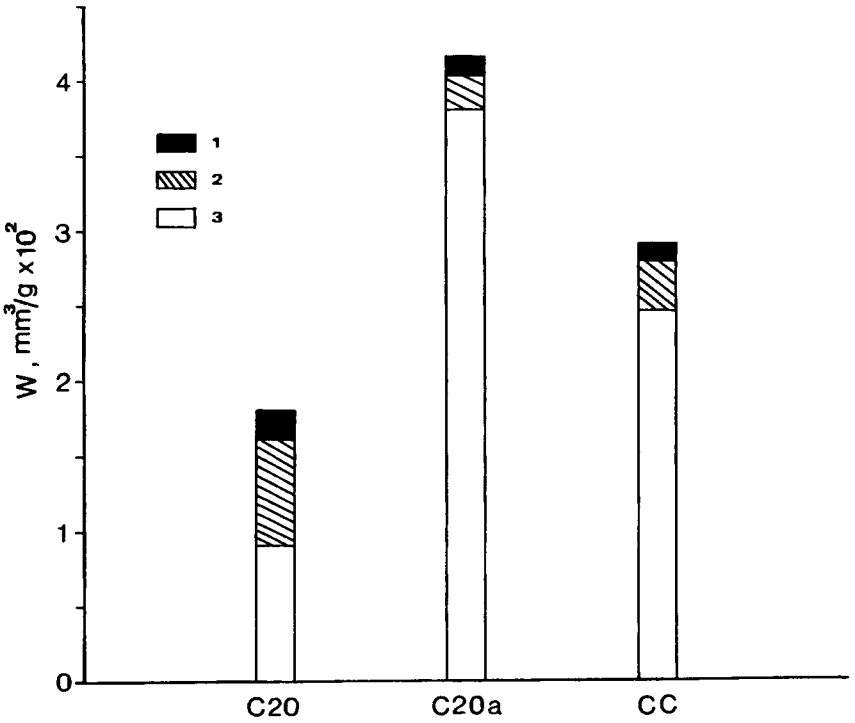

Figure 4 Volume uptake of N_2 at different sizes of pores on adsorbents of Table I: W, liquid volume uptake per mass unit (i.e. cumulative pore volume). The ranges of pore sizes (r, pore radius in Å) are described in Table II. These ranges are approximately: (3) $2.16 < r < 10$ (micropores); (2) $10 < r < 60$; (1) $60 < r < 250$. (The molecular diameter of nitrogen is assumed at 4.33 Å.)

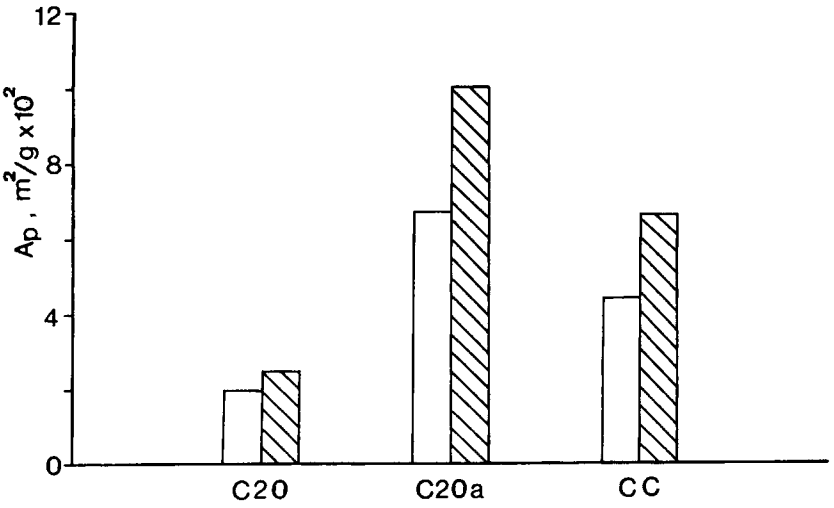

Figure 5 Specific surface area A_p for the adsorption of N_2 on adsorbents (Table I) calculated from the BET isotherm (blank) and the DRK equation (shaded).

The plot of the experimental data of log V versus $\log^2(P/P_o)$ gives a straight line where the intercept is equal to the logarithm of the monolayer capacity (log V_m). Figure 5 represents the specific surface area A_p calculated from the BET isotherm and the DRK equation. For each method, the surface areas of the materials (C20, C20a, CC) have almost the same relation, i.e., both methods give quantitatively corresponding results.

Assuming that the volume of adsorbed vapor of the liquid fill up all the pores with diameter greater than the molecular diameter of the adsorbate molecule, then the pore volume (in cm^3/g) can be calculated from the vapor phase adsorption according to the equation:

$$V_p = X/\rho_L \tag{8}$$

where X is the equilibrium amount of adsorbed pentane per gram solid adsorbent and ρ_L is the density of the adsorbate liquid pentane.

Figure 6 shows the pore volume V_p and the specific surface area A_p calculated from the pentane adsorption results. With increasing values of V_p and A_p, the materials can be ordered C20a > CC > C20.

The statistical thickness t of the adsorbed layers in the case of the adsorption of nitrogen can be determined by the equation[35]:

$$t = 15.47V/S \text{ (Å)} \tag{9}$$

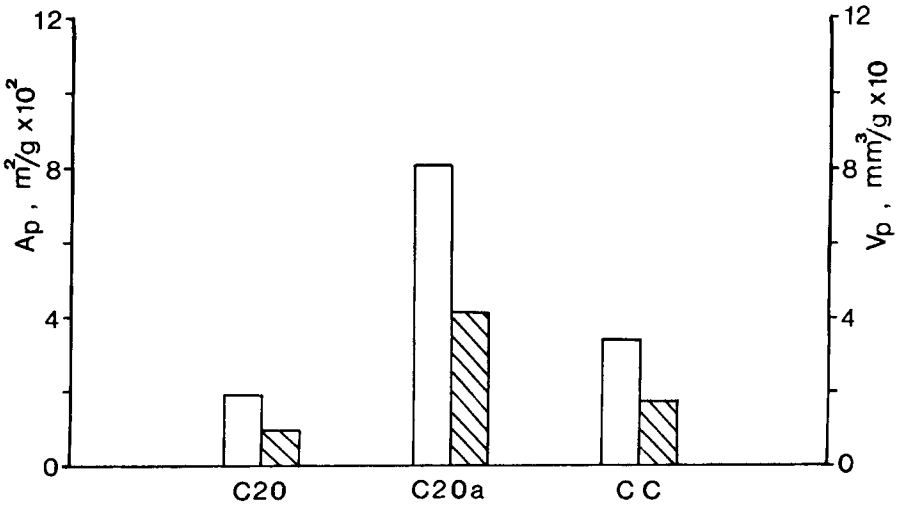

Figure 6 Specific surface area A_p (blank) and pore volume V_p (shaded) for the adsorption of pentane on adsorbents (Table I).

and

$$t = 3.54l \text{ (Å)} \quad (10)$$

where t is the statistical thickness of the adsorbed layer; V is the adsorbed gas volume of the adsorbate in cm^3 gas STP/g of adsorbent (taken at a corresponding relative pressure P/P_o); S is the specific surface area of the adsorbent in m^2/g (commonly taken as the specific surface area from the BET equation); and l is the number of adsorbed layers.

From eq. (10) it follows that for a unimolecular layer the value of t equals 3.54 Å.

The number of layers is referred to in Table II that also summarizes the results of pore volume and pore sizes.

DISCUSSION

The adsorption properties of the materials examined (adsorption capacity, surface area, and pore volume) based on the adsorption of nitrogen and pentane follow the order

$$\text{C20a} > \text{CC} > \text{C20}.$$

The materials can be characterized by the adsorption of nitrogen or pentane, separately. However, the values of pore volume (W_o, W) and A_p determined by the adsorption of nitrogen may deviate from that V_p and A_p by pentane. It is remarkable that C20, which is a less microporous material than C20a and CC, shows the same values of A_p determined by nitrogen (BET method) and pentane as well as the same values of W_o, W determined by nitrogen (DR equation or related to the Kelvin equation at $r_m < 10$ Å), and V_p by pentane. The microporous materials C20a and CC reveal significant deviations in such comparisons. Generally, the values of the specific surface area and the pore volume determined by pentane adsorption is lower than that determined for nitrogen by the DRK and DR equation, respectively. The average area, a_m, occupied by a molecule of pentane is two times or more higher than that of nitrogen as mentioned above. Therefore, more micropores are inaccessible for pentane than the nitrogen molecule.

The micropore volume, W_o, of these materials calculated according to the DR equation is similar to the cumulative volume, W, related to the Kelvin equation for $r_m \leqq \sim 10$ Å (see Table II). The lowest limit of the pore width should be higher than the molecular diameter of nitrogen. In the literature, the molecular diameter of an adsorbate has different values depending on the experimental or calculation method used, e.g., the molecular diameter of nitrogen has the values 3.00, 3.15, 3.53, and 4.33 Å.[35] Assuming the higher value of the molecular diameter of nitrogen, i.e., 4.33 Å, then the nitrogen adsorption corresponds to pore width higher than 4.33 Å.[38]

The micropores contribute to the accessible surface[35] and the micropore volume of active carbons is usually within the range 200–600 mm^3/g, and the most typical values for commercial active carbons are close to 400 mm^3/g.[37] The C20a is close to the latter value of micropore volume, the commercial CC has a lower value, and the only pyrolyzed material, C20, has micropore volume lower than the

Table II Pore Volume and Sizes According to DR and Kelvin Equations Based on Adsorption Isotherms of Nitrogen

No.	Symbol	Micropore Volume, W_o (mm^3/g)	Cumulative Pore Volume, W (mm^3/g)	Pore Radius, r_m ≤(Å)	Relative Pressure, P/P_o	Number of Layers, l
1	C20	93	95	10.78	0.411	
			161	62.54	0.858	
			181	268.86	0.965	2.56
2	C20a	372	380	10.98	0.418	
			402	41.75	0.795	
			414	109.17	0.916	1.70
3	CC	240	244	9.85	0.378	
			278	59.80	0.852	
			291	254.16	0.963	1.86

W_o, total micropore volume; W, cumulative pore volume for corresponding ranges of pore sizes; r_m, pore radius; P and P_o, pressure and saturation pressure, respectively; l, number of layers.

mentioned limits. Therefore, the activation process is necessary for the production of suitable microporous adsorbent.

The mesopores (pore width $2r$: $20 < 2r < 500$ Å) contribute to the specific surface area and the macropores ($2r > 500$ Å) are responsible for the transport of gases and liquid in the system.[34,35] The upper limit of the applicability of the Kelvin equation is r_m about 250 Å and the lower limit is about 10 Å, i.e., it is applicable in the mesopore range.[34] Therefore, the mesopore volume according to Table II is 86 mm^3/g for C20, 34 mm^3/g for C20a, and 47 mm^3/g for CC. The volume of mesopores of common active carbons is relatively small and lies between 20 and 100 mm^3/g,[37] i.e., the mesopore volume of the adsorbents used lies between these values.

The BET model as well as the DR model are criticized in the literature. The BET model[34] assumes that all adsorption sites on the surface are energetically identical, but this is the exception and energetically heterogeneous surfaces are the rule. Furthermore, the model neglects the forces between an adsorbate molecule and its neighbors in the same layer. It is also questionable how far the molecules in all layers after the first should be treated as completely equivalent. The physical adsorption on mesoporous materials can be significantly described by the layer-by-layer filling and the capillary condensation.[34,40] On the other hand, the application of the BET equation to microporous carbons often leads to invalid results.[34–37,39,40]

According to Dubinin, the mechanism of adsorption in very fine pores (micropores) is pore filling rather than layer-by-layer adsorption on the pore walls. For adsorption on some carbons, the DR equation is linear over many orders of magnitude. However, for other carbons deviations from the DR equation are found and in such cases the Dubinin–Astakhov (DA) equation has been proposed in which the exponent 2 in the DR equation is replaced by a third adjustable constant n.[34,39] Another generalization of the DR equation has been proposed by Stoeckli by using other experimental methods also such as immersion calorimetry.[34,41]

The DR equation can be applied for the adsorption of nitrogen on the materials examined in the region of $P/P_o = 0.005$–0.3. These values exceed in both sides the common range (0.01–0.2) for the applicability of the DR equation.[40]

The type I isotherms of the Brunauer classification are characterized by a plateau of the amount adsorbed that is nearly or quite horizontal, and that may cut the $P/P_o = 1$ axis sharply or may show a "tail" as saturation pressure is approached.[34] This shape is observed with highly microporous adsorbents with a much sharper knee at very low relative pressures, because micropores are filled up before a monolayer can be established on the other surface.[35] The nitrogen isotherms of C20a and CC (Fig. 1) follow obviously the type I isotherms. This conclusion confirms also the results of Table II showing mainly the presence of micropores in these materials (high micropore volume).

The type II isotherms are characterized by a continuous increase of the amount adsorbed with increased P/P_o and a sharper increase after a certain value of P/P_o, and it is representative for multilayer adsorption.[34,35] The physical adsorption of gases by nonporous solids gives rise commonly to a type II isotherm. However, the type II is quite compatible with the presence of micropores.[34] The nitrogen isotherm of C20 (Fig. 1) reveals some characteristics of the type II isotherms. However, the sharper increase of its isotherm is near the $P/P_o = 1$; in typical type II isotherms the sharper increase is in intermediate values of P/P_o, e.g., at 0.5. Further, C20 also contains micropores having micropore volume 93 mm^3/g (see Table II). By the activation process of C20 more micropores are developed, or inaccessible to the gas, micropores become more enlarged and the micropore volume is significantly increased (C20a, Table II). Thus, it seems that the nitrogen isotherm of C20 reveals characteristics of both types I and II. Generally, there are many cases of isotherms that are difficult to fit into the classification at all.[34]

The limiting value manifested in the plateau of the type I isotherm exists because the pores are so narrow that they cannot accommodate more than a single molecular layer on their walls. Thus, the plateau represents the filling up of the pores with adsorbate by a process similar to but not identical with capillary condensation and corresponds to the completion of the monolayer.[34] Generally, for a material with pores of every size, the adsorbate is first bound in the micropores at low relative pressure, and every molecule interacts with several wall sites. After the micropores have been filled, adsorption takes place at the external surface at the mesopore and macropore surfaces. The first adsorbate layer is bonded by the interaction between sorbent and sorbate, while bonding of the molecules of the second and subsequent layers depends on the interaction between the adsorbate molecules.[35] According to Table II, the number of layers for 20a and CC is lower than 2. It can be interpreted as the completion of the micropores with a monolayer, but in some mesopores and macropores a second layer can also be formed.

Material C20 contains fewer micropores than both other materials and its number of layers is more than 2. Thus, the mesopores and macropores are covered by two layers or some of them by more layers.

CONCLUSION

The adsorption properties of the materials examined (adsorption capacity, surface area, and pore volume) based on the adsorption of nitrogen and pentane follow the order

$$C20a > CC > C20.$$

The materials can be characterized by the adsorption of nitrogen or pentane, separately. However, the values of V_p and A_p determined by the adsorption of nitrogen may deviate from that by pentane due mainly to the different molecular size of the adsorbates.

The DR equation can be applied for the adsorption of nitrogen on the materials examined in the region of P/P_o = 0.005–0.3, which exceeds in both sides the common range for the applicability of the DR equation.

The activated materials C20a and CC are mainly microporous and reveal the type I isotherms of the Brunauer classification for nitrogen adsorption while the only pyrolyzed material C20 contains both micropores and mesopores and reveals characteristics of both types I and II. The number of layers for 20a and CC is lower than 2, and for C20 is more than 2.

REFERENCES

1. R. Chozick and R. L. Irvin, *Environ. Prog.*, **10,** 282 (1991).
2. D. Chatzopoulos, A. Varma, and R. L. Irvin, *Environ. Prog.*, **13,** 21 (1994).
3. T. K. Ghosh, H. D. Lin, A. L. Hines, *Ind. Eng. Chem. Res.*, **32,** 2390 (1993).
4. H. Jarvelin and J. R. Fair, *Ind. Eng. Chem. Res.*, **32,** 2201 (1993).
5. B. E. Reed, S. Arunachalam, and B. Thomas, *Environ. Prog.*, **13,** 60 (1994).
6. R. M. Taylor and R. W. Kuennen, *Environ. Prog.*, **13,** 65 (1994).
7. G. Madras, C. Erkey, and A. Akgerman, *Environ. Prog.*, **13,** 45 (1994).
8. P. K. T. Liu, *Ind. Eng. Chem. Res.*, **31,** 2216 (1992).
9. U. Eiden and J. Ciprian, *Chem. Ing. Technol.*, **65,** 11, 1329 (1993).
10. J. W. Neely and E. G. Isakoff, *Carbonaceous Adsorbents for the Treatment of Ground and Surface Waters,* Marcel Dekker, New York, Basel, 1982, pp. 41–51.
11. W. F. Wolff, *J. Phys. Chem.*, **62,** 829 (1958).
12. T. G. Lamond, J. E. Metcalff, and P. L. Walker, *Carbon,* **3,** 59 (1965).
13. E. Fitzer and P. Laudenklos, *Proceedings of the International Carbon Conference, Carbon 76,* Baden-Baden, Germany, 1976, p. 80.
14. H. Juntgen, K. Knoblauch, H. Munzner, and W. Peters, *Chem. Ing. Technol.*, **45,** 533 (1973).
15. A. Eichholtz, E. Richter, K. Knoblauch, and H. Juntgen, *Chem. Ing. Technol.*, **57,** 538 (1985).
16. M. Iley, H. Marsh, and F. Rodriguez-Reinoso, *Carbon,* **11,** 683 (1973).
17. J. D. Lopez-Gonzalez, C. Berenguer, and F. Rodriguez-Reinoso, *Proceedings of the International Carbon Conference, Carbon 76,* Baden-Baden, Germany, 1976, p. 63.
18. J. M. Martin-Martinez, M. Molina-Sabio, M. A. Munecas-Vidal, and F. Rodriguez-Reinoso, *Proceedings of the 4th International Carbon Conference, Carbon 86,* Baden-Baden, Germany, Deutsche Keramische Gesellschaft, 1986, p. 298.
19. R. M. Guppy, T. J. Mays, B. McEnaney, F. Rodriguez-Reinoso, and M. Molina-Sabio, *Proceedings of the 4th International Carbon Conference, Carbon 86,* Baden-Baden, Germany, Deutsche Keramische Gesellschaft, 1986, p. 329.
20. K. Periasamy and C. Namasivayan, *Ind. Eng. Chem. Res.*, **33,** 317 (1994).
21. J. Simitzis, *7th International Symposium on Polymers "Polymers 80,"* Varna, Bulgaria, 1980.
22. J. Simitzis, *Angew. Makromol. Chem.*, **153,** 165 (1987).
23. J. Simitzis and J. Sfyrakis, *Angew. Makromol. Chem.*, **163,** 47 (1988).
24. J. Simitzis and J. Sfyrakis, *J. Anal. Appl. Pyrol.*, **26,** 37 (1993).
25. J. Simitzis, *J. Anal. Appl. Pyrol.*, **30,** 161 (1994).
26. J. Simitzis and J. Sfyrakis, *J. Appl. Polym. Sci.*, **54,** 2091 (1994).
27. J. Simitzis and J. Sfyrakis, *Proceedings of the 4th International Carbon Conference, Carbon 86,* Baden-Baden, Germany, Deutsche Keramische Gesellschaft, 1986, p. 505.
28. J. Simitzis and J. Sfyrakis, *J. Appl. Polym. Sci.*, **36,** 1769 (1988).
29. J. Simitzis, *Angew. Makromol. Chem.*, **148,** 41 (1987).
30. J. Simitzis, *Angew. Makromol. Chem.*, **184,** 41 (1991).
31. A. Faliagas, J. Sfyrakis, and J. Simitzis, unpublished data (1994).
32. P. L. Walker, Jr. and J. Janov, in *Hydrophobic Surfaces,* F. M. Fowkes, Ed., Academic Press, New York, London, 1969, p. 108.
33. Encycl. of Polym. Sci. & Techn., Vol. 5, H. F. Mark, N. G. Gaylord, and N. M. Bikales, Eds., Interscience Publ./John Wiley & Sons, New York, London, 1966, pp. 72–74.

34. S. J. Gregg and K. S. W. Sing, *Adsorption, Surface Area and Porosity,* Academic Press, London, New York, 1982, pp. 3, 25, 41–50, 103–113, 164, 195, 221–228.
35. R. S. Mikhail and E. Robens, *Microstructure and Thermal Analysis of Solid Surfaces,* Wiley, New York, 1983, pp. 24, 46–48, 56–58, 80–87, 92–100, 168, 184, 443, 451.
36. M. M. Dubinin, *Chem. Rev.,* **60,** 235 (1960).
37. M. M. Dubinin, in *Chemistry and Physics of Carbon,* Vol. 2, P. L. Walker, Ed., Marcel Dekker, Inc., New York, 1966, p. 51.
38. P. Laudenklos, Ph.D. Thesis, University of Karlsruhe, Germany, 1975.
39. B. McEnaney, *Proceedings of the 4th International Carbon Conference, Carbon 86,* Baden-Baden, Germany, Deutsche Keramische Gesellschaft, 1986, p. 1.
40. H. P. Boehm and H. H. Warnecke, *Proceedings of the International Carbon Conference, Carbon 76,* Baden-Baden, Germany, 1976, p. 76.
41. H. F. Stoeckli, *Proceedings of the 4th International Carbon Conference, Carbon 86,* Baden-Baden, Germany, Deutsche Keramische Gesellschaft, 1986, p. 271.

Received November 23, 1994
Accepted March 21, 1995